

Direct Reprogramming of Fibroblasts into Neural Stem Cells by Defined Factors

Dong Wook Han,^{1,2,7,*} Natalia Tapia,^{1,7} Andreas Hermann,^{3,4} Kathrin Hemmer,⁵ Susanne Höing,¹ Marcos J. Araúzo-Bravo,¹ Holm Zaehres,¹ Guangming Wu,¹ Stefan Frank,¹ Sören Moritz,¹ Boris Greber,¹ Ji Hun Yang,¹ Hoon Taek Lee,² Jens C. Schwamborn,⁵ Alexander Storch,^{3,4} and Hans R. Schöler^{1,6,*}

¹Department of Cell and Developmental Biology, Max Planck Institute for Molecular Biomedicine, Röntgenstrasse 20, 48149 Münster, Germany

²Department of Stem Cell Biology, School of Medicine, SMART Institute of Advanced Biomedical Science, Konkuk University, 1 Hwayang-dong, Gwangjin-gu, Seoul 143-701, Republic of Korea

³Division of Neurodegenerative Diseases, Department of Neurology and Center for Regenerative Therapies Dresden (CRTD), Dresden University of Technology, 01307 Dresden, Germany

⁴German Centre for Neurodegenerative Diseases (DZNE), 01307 Dresden, Germany

⁵Westfälische Wilhelms-Universität Münster, ZMBE, Institute of Cell Biology, Stem Cell Biology and Regeneration Group, Von-Esmarch-Str. 56, 48149 Münster, Germany

⁶Medical Faculty, University of Münster, Domagkstrasse 3, 48149 Münster, Germany

⁷These authors contributed equally to this work

*Correspondence: dwhan@konkuk.ac.kr (D.W.H.), office@mpi-muenster.mpg.de (H.R.S.)

DOI 10.1016/j.stem.2012.02.021

SUMMARY

Recent studies have shown that defined sets of transcription factors can directly reprogram differentiated somatic cells to a different differentiated cell type without passing through a pluripotent state, but the restricted proliferative and lineage potential of the resulting cells limits the scope of their potential applications. Here we show that a combination of transcription factors (*Brn4/Pou3f4*, *Sox2*, *Klf4*, *c-Myc*, plus *E47/Tcf3*) induces mouse fibroblasts to directly acquire a neural stem cell identity—which we term as induced neural stem cells (iNSCs). Direct reprogramming of fibroblasts into iNSCs is a gradual process in which the donor transcriptional program is silenced over time. iNSCs exhibit cell morphology, gene expression, epigenetic features, differentiation potential, and self-renewing capacity, as well as in vitro and in vivo functionality similar to those of wild-type NSCs. We conclude that differentiated cells can be reprogrammed directly into specific somatic stem cell types by defined sets of specific transcription factors.

INTRODUCTION

Transcription factors specific to embryonic stem cells (ESCs) have been described to induce pluripotency in somatic cells (Maherali et al., 2007; Okita et al., 2007; Takahashi et al., 2007; Takahashi and Yamanaka, 2006; Wernig et al., 2007). Recent studies have successfully demonstrated the direct reprogramming of differentiated cells into other differentiated cell types, including neurons, cardiomyocytes, blood progenitor cells, hepatocytes, and epiblast stem cells (Han et al., 2011; Huang

et al., 2011; Ieda et al., 2010; Sekiya and Suzuki, 2011; Szabo et al., 2010; Vierbuchen et al., 2010). However, it is not known whether cell type-specific transcription factors can force somatic cells to acquire different somatic stem cell identities.

Previous studies have shown that combinations of neural transcription factors and/or microRNAs can directly convert both mouse and human fibroblasts into neuronal cells, including dopaminergic and motor neurons (Caiazzo et al., 2011; Marro et al., 2011; Pang et al., 2011; Pfisterer et al., 2011; Son et al., 2011; Vierbuchen et al., 2010; Yoo et al., 2011). The induced neuronal cells showed neuronal-like gene expression patterns and also generated action potentials, indicating that in vitro they are functionally similar to their wild-type counterparts. However, because neurons are not self-renewing cells, limitations exist in obtaining sufficient amounts of cells for both uncovering the mechanisms underlying direct conversion and conducting clinical trials. Neural stem cells (NSCs), a well-characterized somatic stem cell type, are capable of self-renewing, as well as differentiating into their daughter cell types (Reynolds and Weiss, 1992). Therefore, the successful reprogramming of fibroblasts into NSCs, instead of neurons, would provide a potentially unlimited source of neurons and other neural cell types.

Here we show the direct conversion of fibroblasts into functional NSCs with defined factors. Directly reprogrammed NSCs, i.e., induced NSCs (iNSCs), closely resemble brain tissue-derived NSCs in several characteristics, including morphology, expression profile, self-renewing capacity, epigenetic status, and differentiation potential, as well as in vitro and in vivo functionality.

RESULTS

Induction of NSC Fate on Fibroblasts

For the direct reprogramming into NSCs, we used three stem cell factors (*Sox2*, *Klf4*, and *c-Myc*) together with eight neural-specific transcription factors (*Pax6*, *Olig2*, *Brn4/Pou3f4*, *E47/Tcf3*, *Mash1/Ascl1*, *Sip1*, *Ngn2/Neurog2*, plus *Lim3/Lhx3*;

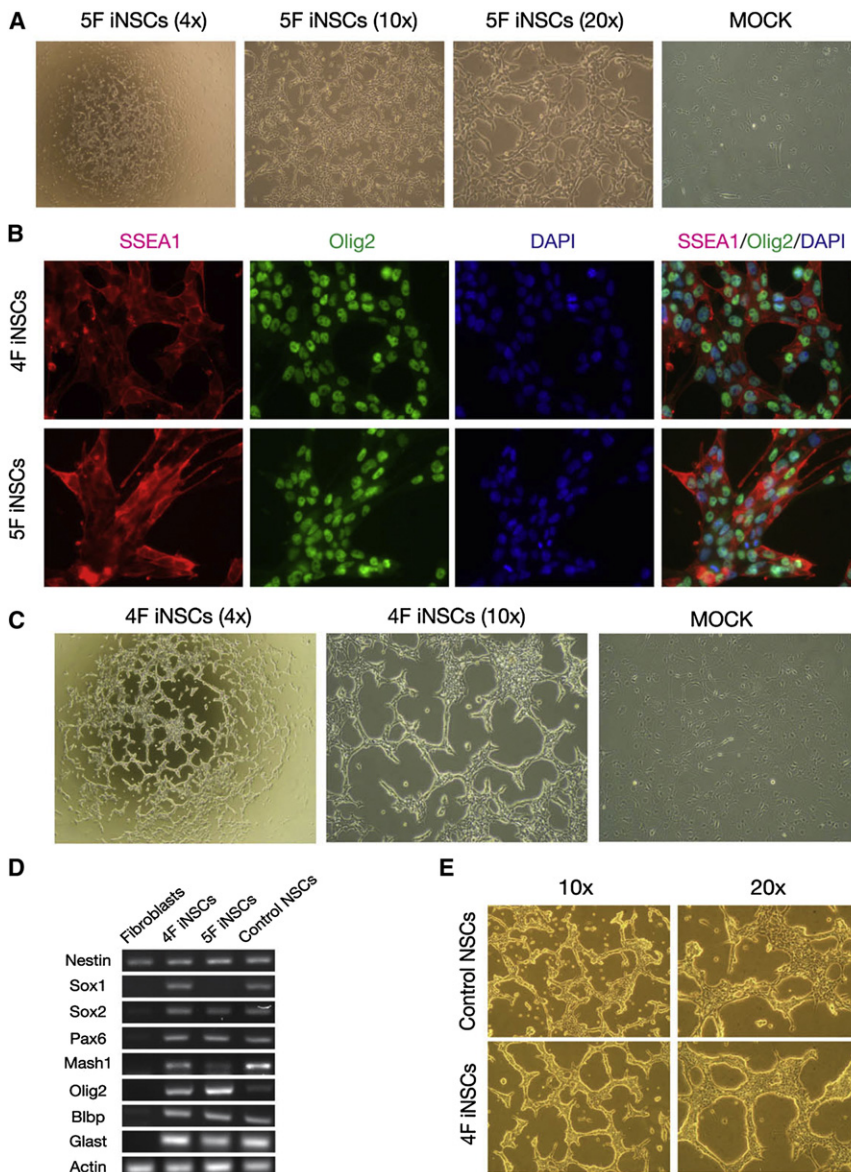


Figure 1. Direct Reprogramming of Fibroblasts into iNSCs

(A) Morphology of an early iNSC cluster generated by a combination of five factors (5F; SKMBE), as assessed by bright-field microscopy. MOCK corresponds to fibroblasts that were not transduced with the reprogramming cocktails but were maintained under NSC culture conditions.

(B) Immunofluorescence microscopy images of control NSCs and iNSCs (4F and 5F), using antibodies against SSEA1 and Olig2.

(C) Morphology of an early iNSC cluster generated by four factors (SKMB), as assessed by bright-field microscopy. MOCK corresponds to fibroblasts that were not transduced with the reprogramming cocktails but were maintained under NSC culture conditions.

(D) RT-PCR analysis showed that both 4F and 5F iNSCs exhibit a gene expression profile similar to that of control NSCs.

(E) 4F iNSCs could be stably maintained for more than 130 passages.

See also Figures S1 and S2 and Table S1.

we omitted *Pax6* and *Olig2* and used *E47*. Within 4–5 weeks of infection with this 5-factor (5F) combination (*Brn4*, *Sox2*, *Klf4*, *c-Myc*, *E47*; BSKME), we obtained 2–5 NSC-like cell clusters (Figure 1A; Table S1), from which we were able to establish stable cell lines that expressed NSC markers, indicating that fibroblasts could be directly reprogrammed into an NSC-like state with defined factors (Figures 1B and S1B). Thus, we tentatively termed these cells “induced NSCs (iNSCs).”

We were able to further scale down the number of factors to four (*Brn4*, *Sox2*, *Klf4*, *c-Myc*; BSKM), but we obtained only 1–3 NSC-like clusters (Table S1). Again, these 4F iNSCs looked very similar to both control NSCs and 5F iNSCs

(BSKME) (Figure 1C). We were also able to generate iNSCs from fibroblasts of different sources (Figures S1C and S1D, Table S1) and showed integration of all transgenes (Figure S2A). Using both immunostaining and reverse transcriptase-polymerase chain reaction (RT-PCR), we found that 4F iNSCs express NSC-specific markers (Figures 1B, 1D, and S1B). iNSCs showed slightly larger nuclei than control NSCs (Figure S1E) and could be maintained for more than 130 passages with proliferation rates slightly higher than control NSCs (Figures 1E and S1F). Importantly, 4F and 5F iNSCs did not generate teratomas after injection into immunosuppressed mice (Figure S1G).

Strikingly, 4F iNSCs showed complete silencing of all transgenes used in the reprogramming experiments. Although transgenic expression of both *c-Myc* and *E47* was not detected in 5F iNSCs, transgenic levels of *Sox2*, *Klf4*, and *Brn4* were detected, albeit at levels lower than in fibroblasts on day 4 postinfection (Figure S2B), indicating a silencing trend. The expression levels of the

SKMPOBEMSNL). After several attempts, we obtained some neuron-like cells, but no NSC-like cells (Table S1 available online). *Ngn2* and *Lim3* are specific for more differentiated cell types, such as motor neurons (Marro et al., 2011), so we excluded *Ngn2* and *Lim3* from our reprogramming cocktail. With the nine remaining factors, we tested a series of seven factor combinations of which three resulted in NSC-like clusters. All three had *Sox2*, *Klf4*, *c-Myc*, *Pax6*, *Olig2*, and *Brn4* (SKMPOB) in common, and the extra factors were either *E47*, *Mash1*, or *Sip1* (SKMPOB-E, -M, -S; Figure S1A, Table S1). However, we could not stably maintain the NSC-like cells from these three combinations, and they eventually differentiated into cells that looked like neurons (data not shown).

We then tested different combinations and also tried to scale down the number of factors in the reprogramming cocktail by using the common factors (SKMPOB) and the three variable factors (EMS). The most promising result was obtained when

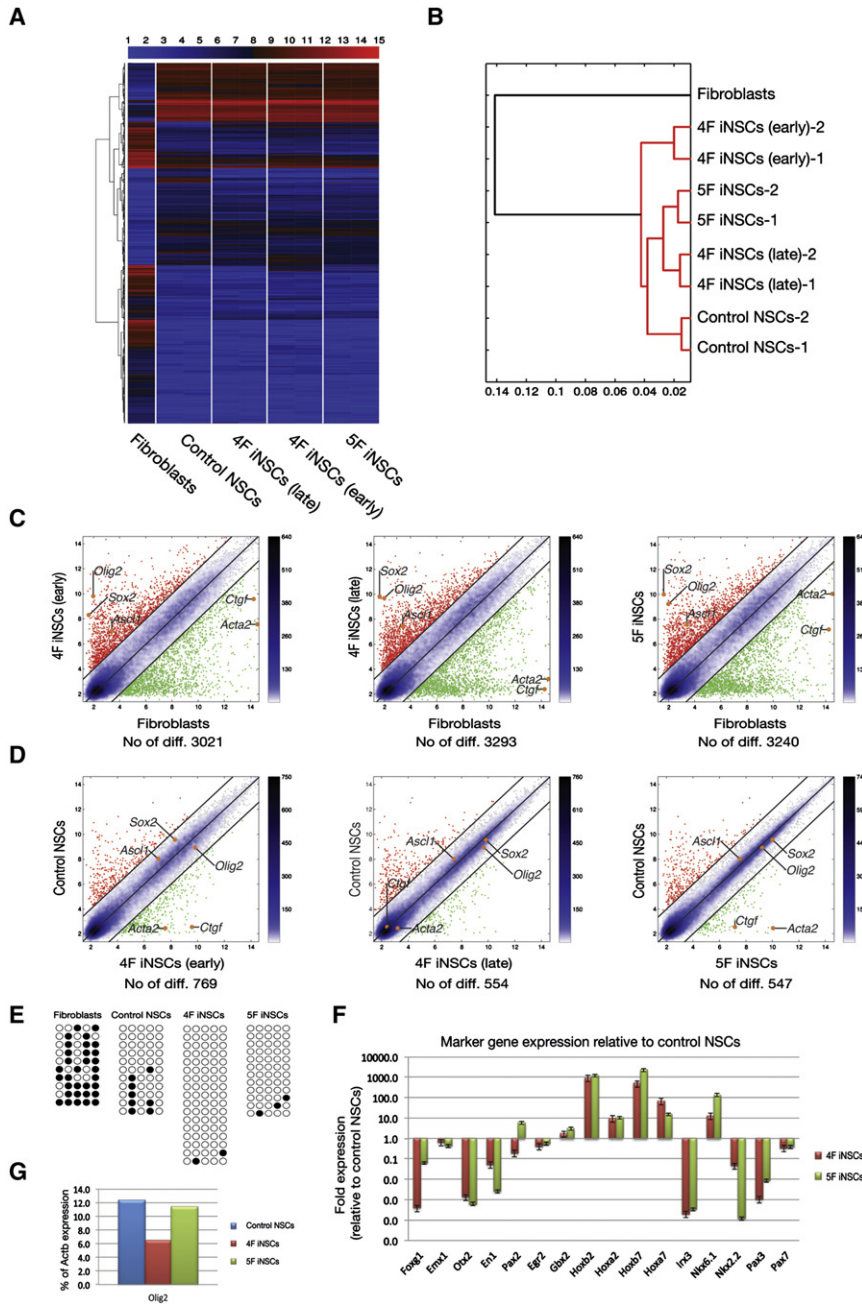


Figure 2. Characterization of iNSCs

(A) Heat map from microarray data demonstrating global gene expression pattern in fibroblasts, control NSCs, 4F iNSCs of early and late passages, and 5F iNSCs. The color bar at the top indicates gene expression in log₂ scale. Red and blue colors represent higher and lower gene expression levels, respectively.

(B) Hierarchical clustering of the cell lines based on the gene expression profiles in (A).

(C and D) Pairwise scatter plot analysis of the global gene expression profiles of 4F iNSCs of early and late passages, and 5F iNSCs versus the parental fibroblasts (C) and control NSCs (D). Black lines indicate boundaries of 2-fold difference in gene expression levels. The bar to the right indicates the scattering density; the higher the scattering density, the darker the blue color. Gene expression levels are depicted in log₂ scale. The number of differentially expressed genes is indicated under each scatter plot.

(E) DNA methylation status on the second intron of *Nestin* in fibroblasts, control NSCs, and 4F and 5F iNSCs was assessed by bisulfite sequencing PCR. Open and filled circles represent unmethylated and methylated CpGs, respectively.

(F) Expression levels of region-specific marker genes. All data are calibrated to the control NSCs, whose expression is considered to be 1 for all genes. Error bars correspond to the normalization against two housekeeping genes.

(G) Expression level of *Olig2* in control NSCs and both 4F and 5F iNSCs as percentage of *Actin* expression.

See also Figure S3 and Table S2.

endogenous factors in both 4F and 5F iNSCs were similar to those of control NSCs, indicating that the exogenous factors had properly activated the endogenous transcriptional network typical for NSCs (Figure S2B). In summary, we successfully generated stable cell lines with two reprogramming cocktails, BSKME and BSKM, and found that these lines highly resemble NSCs in morphology, marker gene expression, and self-renewing capacity.

Direct Conversion of Fibroblasts into iNSCs Is a Gradual Process

We analyzed the whole-genome profile of 5F iNSCs and of early- and a late-passage 4F iNSCs to evaluate the reprogramming

level of the entire transcriptome. The global genome heat map indicates a genome-wide conversion from a fibroblast to an NSC transcriptional program (Figure 2A). Accordingly, both hierarchical clustering analyses and pairwise scatter plots showed that the iNSCs closely resemble the control NSCs but clearly differ from the parental fibroblasts (Figures 2B–2D). iNSCs and control NSCs showed similar expression levels of NSC markers, such as *Olig2*, *Sox2*, and

Mash1/Ascl1, which were not expressed in fibroblasts. Because *Olig2* and *Mash1/Ascl1* were not provided exogenously, this result demonstrates activation of the endogenous NSC program. Fibroblasts, but not control NSCs, exhibited high expression levels of connective tissue marker *Ctgf* (Ivkovic et al., 2003) and the skeletal muscle marker *Acta2* (Schludmeyer et al., 2000). Interestingly, 4F iNSCs of an early passage showed intermediate expression levels of *Ctgf* and *Acta2* but high expression levels of typical NSC markers, such as *Sox2*, *Olig2*, and *Mash1/Ascl1*, that were already comparable to control NSCs (Figures 2C and 2D). 4F iNSCs of a late passage showed further suppression of *Ctgf* and *Acta2* to levels similar to those in NSCs. We

found similar results for several other fibroblast-specific genes (Figure S3A). In addition, early-passage 4F iNSCs showed low expression levels of genes that are highly expressed in control NSCs but not in fibroblasts. However, late-passage 4F iNSCs expressed those genes at levels similar to control NSCs (Figure S3B). These findings demonstrate that reprogramming is a gradual process in which the donor cell type-specific transcriptional program is silenced over a period of time. Furthermore, 5F iNSCs, which were more similar to late-passage 4F iNSCs than to early-passage 4F iNSCs in gene expression, still showed relatively high expression levels of some fibroblast markers, such as *Acta2* and *Ctgf* (Figures 2C, 2D, and S3C). These results indicate that the reprogrammed iNSCs retain the epigenetic memory of the initial donor cell type, in this case connective tissue cells, thus excluding the possibility that neural progenitors are the initial cell type in the conversion process.

The second intron of *Nestin* is unmethylated in *Nestin*-expressing cells, but it is methylated in fibroblasts (Han et al., 2009). Therefore, we assessed its DNA methylation status in parental fibroblasts, control NSCs, and both 4F and 5F iNSCs (Figure 2E). The second intron of *Nestin* was completely unmethylated in 4F and 5F iNSCs, just as in control NSCs, suggesting that reprogramming had also occurred at the epigenetic level.

To determine the regional identity of the generated iNSCs, we analyzed the gene expression level of several markers along the anterior-posterior and dorsal-ventral axes of the brain. Microarray analysis revealed a strong bias toward expression of anterior hindbrain markers (*Gbx2*, *Hoxb2*, *Hoxa2*) and even more so for posterior markers (*Hoxa7*, *Hoxb7*). We did not detect expression of anterior markers, such as *Foxg1*, *Emx1*, and *Otx2* (Dou et al., 1999; Simeone et al., 1992a, 1992b), but detected downregulated, or only weak, expression of midbrain markers, such as *En1* (Table S2; Davis and Joyner, 1988). We validated these microarray data by qRT-PCR (Figure 2F), confirming a bias toward posterior regions, with more than 400-fold higher levels of the marker genes *Hoxb2* and *Hoxb7* (Giampaolo et al., 1989). Along the dorsal-ventral axis, we detected expression of only the ventral hindbrain marker *Nkx6.1*, whereas we detected either no or strongly downregulated expression of other ventral markers, such as *Irx3* and *Nkx2.2* (Briscoe et al., 2000), compared with control NSCs. Notably, we found very high expression of the ventral marker *Olig2*, comparable to control NSCs (Figure 2G), but no expression of the dorsal markers *Pax3* (Goulding et al., 1991) and *Pax7* (Figure 2F; Kawakami et al., 1997). Taking these results together, we suggest a posterior regionalization of the iNSCs, as both 4F and 5F iNSCs showed strong upregulation of posterior marker genes with parallel downregulation of anterior marker genes. Moreover, it is likely that our iNSCs reflect a more ventral position as a result of the expression of the ventral hindbrain gene *Nkx6.1* and high expression of *Olig2*, a gene involved in the development of neurons in the ventral spinal cord (Poh et al., 2002).

iNSCs Are as Functionally Mature as Control NSCs

We then decided to evaluate the functionality of the iNSCs. After inducing the differentiation of both 4F and 5F iNSCs into neurons for 7–16 days (Figure 3A), we found that 4F and 5F iNSCs could be differentiated into neurons that expressed sodium currents

and that were able to generate single as well as multiple action potentials (Figure 3C; Table S3). The multipotency of the 4F (passage 97) and 5F (passage 89) iNSCs was assessed via the cells' ability to differentiate into astrocytes, neurons, and oligodendrocytes, as evidenced by GFAP, Tuj1, and O4 staining, respectively (Figure 3A). Both 4F and 5F iNSC lines were able to form neurons and astrocytes with the same efficiency as control NSCs. However, the differentiation of iNSCs into oligodendrocytes was significantly impaired (Figure 3B). As expected, most neurons were either GABAergic, glutamatergic, or to a lesser extent cholinergic (Figure 3D). Some neurons in control NSCs and differentiated 5F iNSC, but not 4F iNSC, cultures expressed tyrosine hydroxylase (TH), a marker for dopaminergic cells. Neurons from all three NSC types expressed vesicular glutamate transporter 1 (VGLUT1), which packs glutamate into synaptic vesicles, suggesting the development of synapses (Figure 3D). Therefore, no major differences were observed in the neurons generated from control NSCs versus iNSCs in morphology, immunocytochemistry, and functional analyses.

Finally, to assess the in vivo differentiation potential of iNSCs, we transplanted 1.5×10^5 5F iNSCs labeled with green fluorescent protein (GFP) into the subventricular zone of adult mice. Two weeks after transplantation, we analyzed the fate of the transplanted cells in fixed sections (Figure 4A). The grafts typically consisted of a densely packed core, a less densely organized edge of cells, and a fraction of migrating cells that had integrated into the rostral migratory stream (RMS) (Figure 4B). As the cells had been transplanted into the subventricular zone, one of the stem cell niches of the adult brain, we expected that at least some of them would retain their neural stem cell identity. Indeed, we detected GFP-positive cells that also expressed the progenitor marker *Nestin* and the proliferation marker Ki67 (Figures 4C and S4A). Nevertheless, we never detected any cells that were positive for the NSC marker *Sox2* (Figures 4D and S4B), indicating that although some of the transplanted cells maintained a neural progenitor identity for some time, none of them remained as NSCs. During adult neurogenesis, NSCs produce committed neural progenitors, which eventually become neurons. Those progenitor cells express the marker *Mash1*. We found that some of the transplanted iNSCs were positive for nuclear *Mash1* (Figures 4D and S4B), indicating that iNSCs also followed the same sequence of events in the differentiation process as do endogenous NSCs. Those GFP⁺/*Mash1*⁺ cells were mainly localized to the edges of the graft. Originating from those edges, some grafted cells migrated to and integrated into the RMS (Figure 4B). After in vivo differentiation, the migrating cells were found to be positive for the neuronal markers *Dcx* and *TuJ1*, indicating that the grafted cells had committed to the neuronal lineage in vivo (Figures 4E and S4C). Furthermore, the grafted cells had also committed to the glial lineage, as evidenced by the presence of GFP⁺/GFAP⁺ and GFP⁺/NG2⁺ cells (Figures 4E and S4D). Finally, the transplanted iNSCs also had the ability to differentiate into oligodendrocytes, as evidenced by the presence of GFP⁺/*Olig2*⁺ and GFP⁺/*S100β*⁺ cells (Figures 4E and S4E). Taking all these results together, we conclude that iNSCs have the potential to undergo differentiation both in vitro and in vivo into all neural cell lineages.

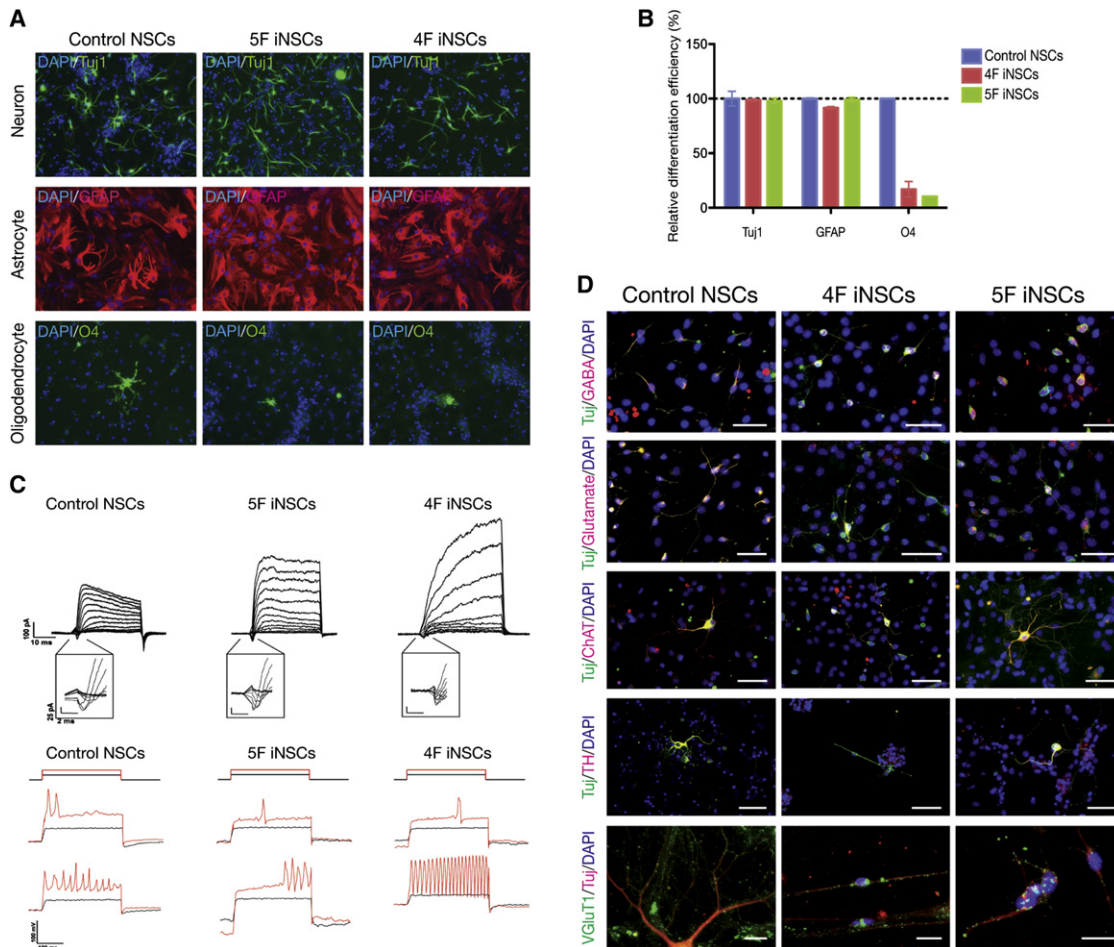


Figure 3. In Vitro Differentiation Potential of iNSCs

(A) Differentiation potential of 4F and 5F iNSCs into neurons, astrocytes, and oligodendrocytes, as determined by immunocytochemistry with antibodies against Tuj1, GFAP, and O4, respectively.

(B) The efficiency of differentiation into neurons, astrocytes, and oligodendrocytes from control NSCs and iNSCs (4F and 5F) was quantified and compared via immunostaining with Tuj1, GFAP, and O4, respectively. Error bars correspond to SEM.

(C) Electrophysiological properties of control NSC- and iNSC-derived neurons. Representative voltage-clamp recordings in response to increasing voltage pulses from neurons derived from control NSCs, 5F iNSCs, and 4F iNSCs after 7–16 days of differentiation. Insets represent higher magnification of sodium currents. Both single and multiple action potentials were detected in neurons derived from control NSCs, 5F iNSCs, and 4F iNSCs.

(D) Characterization of neurons derived from control NSCs and iNSCs. Representative immunofluorescence images of differentiated control NCS, 4F iNSCs, and 5F NSCs after 14–21 days of differentiation. All three NSC types behaved similarly in spontaneous differentiation behavior and differentiated into all major neuronal subtypes, namely GABAergic and glutamatergic neurons, ChAT⁺ cholinergic and TH⁺ dopaminergic neurons (except that 4F iNSCs did not differentiate into TH⁺ neurons). Dotted VGlut1 expression in proximity of Tuj1⁺ nerve fibers suggested morphological synapse formation. Scale bars represent 50 μ m and 20 μ m (lowermost panel). ChAT, choline acetyltransferase; TH, tyrosine hydroxylase; Tuj, β -tubulin class III; VGlut1, vesicular glutamate transporter type 1.

See also Table S3.

DISCUSSION

In this study, we show direct reprogramming of fibroblasts into a self-renewing somatic stem cell type. With a defined set of factors, we successfully generated iNSCs that have the ability to self-renew and are nearly identical to control NSCs in morphology, gene expression profile, epigenetic features, and even in vitro and in vivo functionality. Remarkably, the iNSCs can be engrafted in the stem cell niches of the mouse adult brain, where they can not only continue to proliferate, but also differentiate into neurons, astrocytes, and oligodendrocytes, demonstrating a bona fide multipotency in vivo and suggesting potential

therapeutic applications. Although the reprogrammed iNSCs were able to suppress the fibroblast-specific transcription network, they still maintained some epigenetic memory of the initial donor cell. Nevertheless, the remaining somatic signature did not impair the functionality of iNSCs both in vitro and in vivo. These results suggest that the newly established NSC transcriptional network is dominant over the remaining fibroblast program. Furthermore, the transcriptional profiling of the same 4F iNSC clone at both early and late passages has provided very interesting insights into the dynamics of somatic memory erasure and establishment of the new transcriptional network, demonstrating that reprogramming is a gradual process.

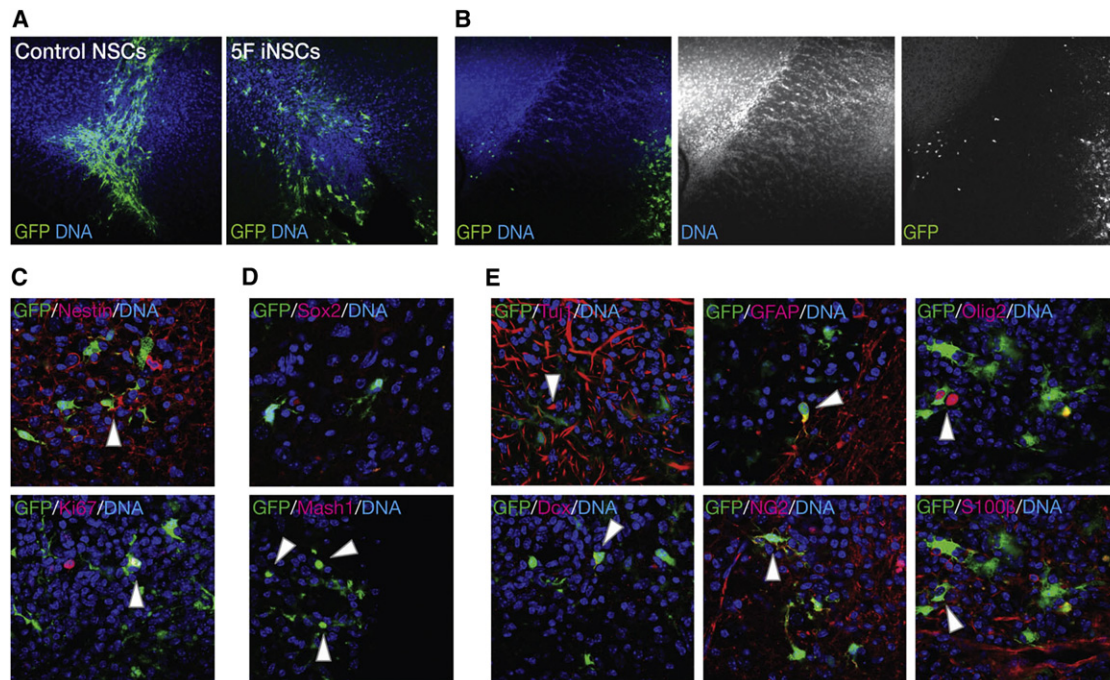


Figure 4. iNSCs Are Functionally Similar to Control NSCs

(A) In vivo transplantation of iNSCs. 1.5×10^5 5F iNSCs labeled with GFP were stereotactically transplanted into the subventricular zone of an adult mouse. After transplantation, the fate of transplanted iNSCs was analyzed.

(B) Injected cells migrate from the graft into the rostral migratory stream.

(C) Some of the transplanted cells remained as progenitors, as indicated by the presence of the marker Nestin. Some of the injected cells also maintained the ability to proliferate, as shown by Ki67 staining.

(D) Transplanted iNSCs became Sox2⁺ but Mash1⁻, suggesting that the iNSCs did not remain as NSCs, but had differentiated.

(E) The transplanted iNSCs showed differentiation into neurons (GFP⁺/Tuj1⁺/Dcx⁺), astrocytes (GFP⁺/GFAP⁺/NG2⁺), and oligodendrocytes (GFP⁺/S100 β ⁺/Olig2⁺), as determined by immunohistochemistry (E).

See also Figure S4.

Recently, Kim et al. (2011) successfully reprogrammed fibroblasts into neural progenitor cells (NPCs). The generated NPCs could be expanded for only a few passages, thus excluding the possibility that the cells have a permanent self-renewing capacity—a critical requirement for the clinical applicability of somatic stem cells. Moreover, because these authors used *Oct4* in their reprogramming cocktail, the possibility could not be excluded that the OSKM cocktail had partially reprogrammed the fibroblasts toward an intermediate pluripotent cell state before the culture conditions kicked in to determine the neural precursor fate (Kim et al., 2011). In contrast, in our study, we omitted *Oct4* from the reprogramming cocktail and thus described the direct reprogramming of fibroblasts into NSCs—i.e., without the cells first passing through an intermediate pluripotent stage. Although *Brrn4* is a member of the POU factor family, it could not replace *Oct4* in iPSC generation, excluding the possibility that iNSCs were generated via the differentiation of iPSCs (data not shown). Lujan et al. (2012) recently reported the generation of self-renewing induced neural precursor cells (iNPCs). However, iNPCs could not be stably maintained in the absence of doxycycline-mediated ectopic expression of factors.

Because we had used nontransgenic fibroblasts, we could not accurately determine the efficiency of iNSC generation. The generation of iNSCs with NSC-specific reporter cell lines would

certainly enhance our understanding of the kinetics of the direct reprogramming process. It would also be interesting to determine whether the use of the same reprogramming cocktail could induce both mouse adult cells and human somatic cells to acquire an NSC identity. Although iNSCs exhibited differentiation potential both in vivo and in vitro, we did not observe spontaneous synaptic activity. Therefore, both the functional synaptogenesis and neuronal integration of iNSC-derived neurons must be demonstrated in future studies. Various studies have recently described the induction of pluripotency without the use of viruses and their subsequent integration into the host DNA—i.e., by using recombinant proteins, plasmids, messenger RNAs, and microRNAs to deliver key reprogramming factors (Anokye-Danso et al., 2011; Kim et al., 2009; Okita et al., 2008; Stadtfeld et al., 2008; Warren et al., 2010; Zhou et al., 2009). Future studies should aim to develop new methods for the effective generation of clinical-grade iNSCs and ultimately for the application of these procedures in the clinical setting.

EXPERIMENTAL PROCEDURES

Generation of iNSCs

To generate iNSCs, fibroblasts (5×10^4 cells) were infected with pMX retrovirus expressing the reprogramming factors in different combinations for 48 hr. Cells were cultured in standard NSC medium: DMEM/F-12

supplemented with N2 or B27 (GIBCO-BRL), 10 ng/ml EGF, 10 ng/ml bFGF (both from Invitrogen), 50 μ g/ml BSA (Fraction V; GIBCO-BRL), and 1 \times penicillin/streptomycin/glutamine (GIBCO-BRL). After we observed the first mature iNSC clusters, we either manually picked a mature iNSC clump or passaged and seeded whole dishes of cells onto either gelatin- or laminin-coated dishes and changed the medium every 24 hr. Animal handling was in accordance with the MPI animal protection guidelines and the German animal protection laws.

ACCESSION NUMBERS

The microarray data are available in the Gene Expression Omnibus (GEO) database (<http://www.ncbi.nlm.nih.gov/gds>) under the accession number GSE30500.

SUPPLEMENTAL INFORMATION

Supplemental Information includes Supplemental Experimental Procedures, four figures, and three tables and can be found with this article online at [doi:10.1016/j.stem.2012.02.021](https://doi.org/10.1016/j.stem.2012.02.021).

ACKNOWLEDGMENTS

This research was supported by the Max Planck Society; the Basic Science Research Program through the National Research Foundation of Korea (NRF) funded by the Ministry of Education, Science and Technology (2011-0013885); and the Bio & Medical Technology Development Program of the National Research Foundation (NRF) funded by the Korean government (MEST) (2011-0019490). We are grateful to Areti Malapetsas for editing the manuscript. D.W.H. and H.R.S. designed the experiments. D.W.H., A.H., N.T., K.H., S.H., H.Z., S.F., B.G., S.M., and J.H.Y. performed the experiments. D.W.H., A.H., N.T., S.H., M.J.A.-B., S.F., S.M., H.T.L., J.C.S., and A.S. analyzed the data. D.W.H., N.T., and H.R.S. wrote the manuscript.

Received: November 14, 2011

Revised: January 27, 2012

Accepted: February 24, 2012

Published online: March 22, 2012

REFERENCES

- Anokye-Danso, F., Trivedi, C.M., Jühr, D., Gupta, M., Cui, Z., Tian, Y., Zhang, Y., Yang, W., Gruber, P.J., Epstein, J.A., and Morrisey, E.E. (2011). Highly efficient miRNA-mediated reprogramming of mouse and human somatic cells to pluripotency. *Cell Stem Cell* 8, 376–388.
- Briscoe, J., Pierani, A., Jessell, T.M., and Ericson, J. (2000). A homeodomain protein code specifies progenitor cell identity and neuronal fate in the ventral neural tube. *Cell* 101, 435–445.
- Caiazzo, M., Dell'Anno, M.T., Dvoretzskova, E., Lazarevic, D., Taverna, S., Leo, D., Sotnikova, T.D., Menegon, A., Roncaglia, P., Colciago, G., et al. (2011). Direct generation of functional dopaminergic neurons from mouse and human fibroblasts. *Nature* 476, 224–227.
- Davis, C.A., and Joyner, A.L. (1988). Expression patterns of the homeo box-containing genes *En-1* and *En-2* and the proto-oncogene *int-1* diverge during mouse development. *Genes Dev.* 2 (12B), 1736–1744.
- Dou, C.L., Li, S., and Lai, E. (1999). Dual role of brain factor-1 in regulating growth and patterning of the cerebral hemispheres. *Cereb. Cortex* 9, 543–550.
- Giampaolo, A., Acampora, D., Zappavigna, V., Pannese, M., D'Esposito, M., Carè, A., Faiella, A., Stornaiuolo, A., Russo, G., Simeone, A., et al. (1989). Differential expression of human HOX-2 genes along the anterior-posterior axis in embryonic central nervous system. *Differentiation* 40, 191–197.
- Goulding, M.D., Chalepakis, G., Deutsch, U., Erselius, J.R., and Gruss, P. (1991). Pax-3, a novel murine DNA binding protein expressed during early neurogenesis. *EMBO J.* 10, 1135–1147.
- Han, D.W., Do, J.T., Araúzo-Bravo, M.J., Lee, S.H., Meissner, A., Lee, H.T., Jaenisch, R., and Schöler, H.R. (2009). Epigenetic hierarchy governing Nestin expression. *Stem Cells* 27, 1088–1097.
- Han, D.W., Greber, B., Wu, G., Tapia, N., Araúzo-Bravo, M.J., Ko, K., Bernemann, C., Stehling, M., and Schöler, H.R. (2011). Direct reprogramming of fibroblasts into epiblast stem cells. *Nat. Cell Biol.* 13, 66–71.
- Huang, P., He, Z., Ji, S., Sun, H., Xiang, D., Liu, C., Hu, Y., Wang, X., and Hui, L. (2011). Induction of functional hepatocyte-like cells from mouse fibroblasts by defined factors. *Nature* 475, 386–389.
- Ieda, M., Fu, J.D., Delgado-Olguin, P., Vedantham, V., Hayashi, Y., Bruneau, B.G., and Srivastava, D. (2010). Direct reprogramming of fibroblasts into functional cardiomyocytes by defined factors. *Cell* 142, 375–386.
- Ivkovic, S., Yoon, B.S., Popoff, S.N., Safadi, F.F., Libuda, D.E., Stephenson, R.C., Daluiski, A., and Lyons, K.M. (2003). Connective tissue growth factor coordinates chondrogenesis and angiogenesis during skeletal development. *Development* 130, 2779–2791.
- Kawakami, A., Kimura-Kawakami, M., Nomura, T., and Fujisawa, H. (1997). Distributions of PAX6 and PAX7 proteins suggest their involvement in both early and late phases of chick brain development. *Mech. Dev.* 66, 119–130.
- Kim, D., Kim, C.H., Moon, J.I., Chung, Y.G., Chang, M.Y., Han, B.S., Ko, S., Yang, E., Cha, K.Y., Lanza, R., and Kim, K.S. (2009). Generation of human induced pluripotent stem cells by direct delivery of reprogramming proteins. *Cell Stem Cell* 4, 472–476.
- Kim, J., Efe, J.A., Zhu, S., Talantova, M., Yuan, X., Wang, S., Lipton, S.A., Zhang, K., and Ding, S. (2011). Direct reprogramming of mouse fibroblasts to neural progenitors. *Proc. Natl. Acad. Sci. USA* 108, 7838–7843.
- Lujan, E., Chanda, S., Ahlenius, H., Südhof, T.C., and Wernig, M. (2012). Direct conversion of mouse fibroblasts to self-renewing, tripotent neural precursor cells. *Proc. Natl. Acad. Sci. USA* 109, 2527–2532.
- Maherali, N., Sridharan, R., Xie, W., Utikal, J., Eminli, S., Arnold, K., Stadtfeld, M., Yachechko, R., Tchieu, J., Jaenisch, R., et al. (2007). Directly reprogrammed fibroblasts show global epigenetic remodeling and widespread tissue contribution. *Cell Stem Cell* 1, 55–70.
- Marro, S., Pang, Z.P., Yang, N., Tsai, M.C., Qu, K., Chang, H.Y., Südhof, T.C., and Wernig, M. (2011). Direct lineage conversion of terminally differentiated hepatocytes to functional neurons. *Cell Stem Cell* 9, 374–382.
- Okita, K., Ichisaka, T., and Yamanaka, S. (2007). Generation of germline-competent induced pluripotent stem cells. *Nature* 448, 313–317.
- Okita, K., Nakagawa, M., Hyenjong, H., Ichisaka, T., and Yamanaka, S. (2008). Generation of mouse induced pluripotent stem cells without viral vectors. *Science* 322, 949–953.
- Pang, Z.P., Yang, N., Vierbuchen, T., Ostermeier, A., Fuentes, D.R., Yang, T.Q., Citri, A., Sebastiano, V., Marro, S., Südhof, T.C., and Wernig, M. (2011). Induction of human neuronal cells by defined transcription factors. *Nature* 476, 220–223.
- Pfisterer, U., Kirkeby, A., Torper, O., Wood, J., Nelander, J., Dufour, A., Björklund, A., Lindvall, O., Jakobsson, J., and Parmar, M. (2011). Direct conversion of human fibroblasts to dopaminergic neurons. *Proc. Natl. Acad. Sci. USA* 108, 10343–10348.
- Poh, A., Karunaratne, A., Kolle, G., Huang, N., Smith, E., Starkey, J., Wen, D., Wilson, I., Yamada, T., and Hargrave, M. (2002). Patterning of the vertebrate ventral spinal cord. *Int. J. Dev. Biol.* 46, 597–608.
- Reynolds, B.A., and Weiss, S. (1992). Generation of neurons and astrocytes from isolated cells of the adult mammalian central nervous system. *Science* 255, 1707–1710.
- Schildmeyer, L.A., Braun, R., Taffet, G., Debiassi, M., Burns, A.E., Bradley, A., and Schwartz, R.J. (2000). Impaired vascular contractility and blood pressure homeostasis in the smooth muscle alpha-actin null mouse. *FASEB J.* 14, 2213–2220.
- Sekiya, S., and Suzuki, A. (2011). Direct conversion of mouse fibroblasts to hepatocyte-like cells by defined factors. *Nature* 475, 390–393.
- Simeone, A., Acampora, D., Gulisano, M., Stornaiuolo, A., and Boncinelli, E. (1992a). Nested expression domains of four homeobox genes in developing rostral brain. *Nature* 358, 687–690.
- Simeone, A., Gulisano, M., Acampora, D., Stornaiuolo, A., Rambaldi, M., and Boncinelli, E. (1992b). Two vertebrate homeobox genes related to the

- Drosophila* empty spiracles gene are expressed in the embryonic cerebral cortex. *EMBO J.* 11, 2541–2550.
- Son, E.Y., Ichida, J.K., Wainger, B.J., Toma, J.S., Rafuse, V.F., Woolf, C.J., and Eggan, K. (2011). Conversion of mouse and human fibroblasts into functional spinal motor neurons. *Cell Stem Cell* 9, 205–218.
- Stadtfeld, M., Nagaya, M., Utikal, J., Weir, G., and Hochedlinger, K. (2008). Induced pluripotent stem cells generated without viral integration. *Science* 322, 945–949.
- Szabo, E., Rampalli, S., Risueño, R.M., Schnerch, A., Mitchell, R., Fiebig-Comyn, A., Leivadoux-Martin, M., and Bhatia, M. (2010). Direct conversion of human fibroblasts to multilineage blood progenitors. *Nature* 468, 521–526.
- Takahashi, K., and Yamanaka, S. (2006). Induction of pluripotent stem cells from mouse embryonic and adult fibroblast cultures by defined factors. *Cell* 126, 663–676.
- Takahashi, K., Tanabe, K., Ohnuki, M., Narita, M., Ichisaka, T., Tomoda, K., and Yamanaka, S. (2007). Induction of pluripotent stem cells from adult human fibroblasts by defined factors. *Cell* 131, 861–872.
- Vierbuchen, T., Ostermeier, A., Pang, Z.P., Kokubu, Y., Südhof, T.C., and Wernig, M. (2010). Direct conversion of fibroblasts to functional neurons by defined factors. *Nature* 463, 1035–1041.
- Warren, L., Manos, P.D., Ahfeldt, T., Loh, Y.H., Li, H., Lau, F., Ebina, W., Mandal, P.K., Smith, Z.D., Meissner, A., et al. (2010). Highly efficient reprogramming to pluripotency and directed differentiation of human cells with synthetic modified mRNA. *Cell Stem Cell* 7, 618–630.
- Wernig, M., Meissner, A., Foreman, R., Brambrink, T., Ku, M., Hochedlinger, K., Bernstein, B.E., and Jaenisch, R. (2007). In vitro reprogramming of fibroblasts into a pluripotent ES-cell-like state. *Nature* 448, 318–324.
- Yoo, A.S., Sun, A.X., Li, L., Shcheglovitov, A., Portmann, T., Li, Y., Lee-Messer, C., Dolmetsch, R.E., Tsien, R.W., and Crabtree, G.R. (2011). MicroRNA-mediated conversion of human fibroblasts to neurons. *Nature* 476, 228–231.
- Zhou, H., Wu, S., Joo, J.Y., Zhu, S., Han, D.W., Lin, T., Trauger, S., Bien, G., Yao, S., Zhu, Y., et al. (2009). Generation of induced pluripotent stem cells using recombinant proteins. *Cell Stem Cell* 4, 381–384.